Unanimous Model for Describing the Fast Bioluminescence Kinetics of Ca^{2+}-regulated Photoproteins of Different Organisms

Eremeeva, E. V., Bartsev, S. I., van Berkel, W. J. H., & Vysotski, E. S.

This article is made publically available in the institutional repository of Wageningen University and Research, under article 25fa of the Dutch Copyright Act, also known as the Amendment Taverne.

Article 25fa states that the author of a short scientific work funded either wholly or partially by Dutch public funds is entitled to make that work publicly available for no consideration following a reasonable period of time after the work was first published, provided that clear reference is made to the source of the first publication of the work.

For questions regarding the public availability of this article, please contact openscience.library@wur.nl.

Please cite this publication as follows:

Eremeeva, E. V., Bartsev, S. I., van Berkel, W. J. H., & Vysotski, E. S. (2017). Unanimous Model for Describing the Fast Bioluminescence Kinetics of Ca2+-regulated Photoproteins of Different Organisms. Photochemistry and Photobiology, 93(2), 495-502. https://doi.org/10.1111/php.12664

Photochemistry and Photobiology, 2017, 93: 495–502

Unanimous Model for Describing the Fast Bioluminescence Kinetics of Ca^{2+}-regulated Photoproteins of Different Organisms†

Elena V. Eremeeva[1,‡], Sergey I. Bartsev[2,‡], Willem J. H. van Berkel[3] and Eugene S. Vysotski[1]*

[1]Photobiology Laboratory, Institute of Biophysics SB RAS, Federal Research Center "Krasnoyarsk Science Center SB RAS", Krasnoyarsk, Russia
[2]Theoretical Biophysics Laboratory, Institute of Biophysics SB RAS, Federal Research Center "Krasnoyarsk Science Center SB RAS", Krasnoyarsk, Russia
[3]Laboratory of Biochemistry, Wageningen University & Research, Wageningen, The Netherlands

Received 30 August 2016, accepted 29 September 2016, DOI: 10.1111/php.12664

ABSTRACT

Upon binding their metal ion cofactors, Ca^{2+}-regulated photoproteins display a rapid increase of light signal, which reaches its peak within milliseconds. In the present study, we investigate bioluminescence kinetics of the entire photoprotein family. All five recombinant hydromedusan Ca^{2+}-regulated photoproteins—aequorin from *Aequorea victoria*, clytin from *Clytia gregaria*, mitrocomin from *Mitrocoma cellularia* and obelins from *Obelia longissima* and *Obelia geniculata*—demonstrate the same bioluminescent kinetics pattern. Based on these findings, for the first time we propose a unanimous kinetic model describing the bioluminescence mechanism of Ca^{2+}-regulated photoproteins.

INTRODUCTION

Bioluminescence of a great number of marine organisms, mostly coelenterates, is due to the presence of Ca^{2+}-regulated photoproteins, members of the EF-hand Ca^{2+}-binding protein superfamily. Ca^{2+}-regulated photoproteins are composed of a single polypeptide chain (~22 kDa) to which the oxygenated coelenterazine, 2-hydroperoxycoelenterazine, is tightly bound (1–3). The light-emitting reaction of these photoproteins is triggered by calcium binding to Ca^{2+}-binding loops that initiates oxidative decarboxylation of the 2-hydroperoxycoelenterazine leading to the formation of a product, coelenteramide, in excited state which transition to ground state is accompanied by photon emission. The bioluminescence spectra of the emitted light are broad with maxima around 465–495 nm depending on the type of photoprotein (4).

Despite the fact that Ca^{2+}-regulated photoproteins have been found in many (>25) marine coelenterates (5), cloning and sequence analysis have been carried out only for several aequorins from different species of *Aequorea* (6–10), two clytins (11–14) and two obelins (15–17) from different species of *Clytia* and *Obelia*, respectively, mitrocomins from jellyfish *Mitrocoma cellularia* (18,19) and three light-sensitive Ca^{2+}-regulated photoproteins of ctenophores (20–23), which are functionally identical but reveal no identity of amino acid sequences to hydromedusan photoproteins. Recombinant apophotoprotein can be converted into active photoprotein by incubating with synthetic coelenterazine under Ca^{2+}-free conditions in the presence of O_2 and reducing agents (24). Of note is that apophotoprotein binds coelenterazine on millisecond timescale (25), whereas subsequent conversion of coelenterazine into 2-hydroperoxy adduct is much slower (26).

Although Ca^{2+}-regulated photoproteins represent a unique class of protein biochemistry, in essence, an interest to these proteins is due to their broad analytical potential. The main analytical applications of photoproteins originate from their ability to emit light upon Ca^{2+} binding. Aequorin was the first indicator protein that allowed the quantitative detection of calcium transients in living cells (27). The cDNA cloning of photoprotein genes (28) opened new avenues for their use: Recombinant apophotoprotein is expressed intracellularly, and then coelenterazine added externally diffuses into the cell forming an active photoprotein (29). This approach is highly valuable, because it does not require laborious procedures like microinjection or liposome-mediated transfer of photoprotein into cells. Although Ca^{2+}-regulated photoproteins, mostly aequorin, are still indicators of choice for many applications (30), they are experiencing high competition from fluorescent tetracarboxylate calcium probes (31) and genetically encoded calcium indicators based on green fluorescent protein (32,33).

In the past decade owing to determination of spatial structures of ligand-dependent conformational photoprotein states (2,3,34–36), spatial structures of photoprotein variants (37–39) and comprehensive mutagenesis studies (40–43), significant progress has been attained in understanding the function of certain active site residues in oxidative decarboxylation of 2-hydroperoxycoelenterazine and emitter formation. At the same time, the reason why hydromedusan photoproteins revealing a high degree of sequence and structural identity display different bioluminescent kinetics and sensitivity to calcium (44) still remains an enigma.

Several reaction schemes and models for photoprotein bioluminescence response to Ca^{2+} addition and dependence of bioluminescence on Ca^{2+} concentration were proposed (44–49). According to the kinetic scheme originally suggested for aequorin from *Aequorea victoria* (45), the bioluminescence reaction starts with fast binding of calcium (Scheme 1). With

*Corresponding author e-mail: eugene.vysotski@gmail.com (Eugene S. Vysotski)
†This article is a part of the Special Issue devoted to various aspects of basic and applied research on Bioluminescence.
‡These authors contributed equally to this work.
© 2016 The American Society of Photobiology

calcium concentration at its effective maximum, putative intermediate X is formed. This step is controlled by rate constant k_2, which characterizes the decay phase of photoprotein light signal and represents all chemical transformations of the substrate including 2,3-dioxetanone generation and its subsequent breakdown. Next, intermediate X transforms into an excited singlet state Y*, and this step is independent of calcium and controlled by k_3, which corresponds to the rate constant characterizing the rise phase of photoprotein light signal. Since lifetimes of excited singlet states are typically in the nanoseconds time frame, the value for k_4 is much higher than for the other rate constants.

Photoprotein reaction schemes proposed later were more focused on the relations between light emission and calcium concentration for aequorin and included different numbers of calcium-binding sites which must be occupied to produce bioluminescence (46,47). A simplified but more complete scheme of photoprotein bioluminescence reaction (Scheme 2) was proposed later on the basis of kinetic studies of obelin as well as of stoichiometric observations (48). This scheme accommodated interactions between obelin and various ions such as Ca^{2+}, Mg^{2+}, H^+, K^+ and Na^+.

The next major study of calcium dependence of aequorin bioluminescence made an attempt to correlate the variations of photoprotein decay rates with calcium concentration and the light intensity (49). A parallel model was proposed postulating that the fast and slow light-emitting states coexist and their ratio depends on calcium concentration (Scheme 3). However, the given kinetic scheme does not explain the observed relations between these "fast" and "slow" rate constants and calcium concentration. It was clearly shown that when calcium concentration increased, the "slow" rate constant was decreasing and the "fast" rate constant remained more or less unaffected. One plausible explanation offered was that one of the rate constants on the "slow" reaction pathway depends on the number of calcium ions bound (49).

None of the reaction models of aequorin and obelin bioluminescence proposed so far has been extended to the entire family of Ca^{2+}-regulated photoproteins. Overall, the kinetic model must describe the rise phase of the photoprotein bioluminescence signal and take into account the fact that for most photoproteins, the decay kinetics can be satisfactory described only by two-exponential function. In this study, we present a kinetic model which properly describes full bioluminescence traces of five hydromedusan Ca^{2+}-regulated photoproteins—aequorin from *A. victoria*, clytin from *Clytia gregaria*, mitrocomin from *Mitrocoma cellularia* and obelins from *Obelia longissima* and *Obelia geniculata*.

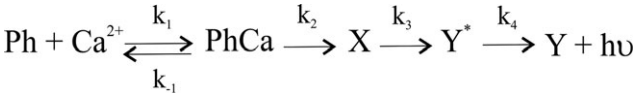

Scheme 1. Proposed reaction scheme for aequorin bioluminescence (45).

MATERIALS AND METHODS

Protein expression and purification. Recombinant apophotoproteins were purified from inclusion bodies and activated with coelenterazine to produce active photoproteins as previously reported (17,50). The coelenterazine concentration was determined using $\varepsilon_{435\ nm}$ = 9800 $cm^{-1}\ M^{-1}$ as molar absorption coefficient (5).

Stopped-flow measurements. Stopped-flow experiments were performed with EDTA-free solutions of photoproteins. EDTA was removed from the purified proteins by gel filtration on a 1.5 × 6.5 cm D-Salt Dextran Desalting column (Pierce). The column was equilibrated and the protein was eluted with 150 mM KCl, 5 mM piperazine-1,4-bis (2-ethanesulfonic acid) (PIPES), pH 7.0 previously passed (twice) through freshly washed beds of Chelex 100 chelating resin (Sigma) to remove trace amounts of Ca^{2+}. The fractions containing photoproteins were identified by bioluminescence assay. To avoid possible contamination with EDTA, only the first few protein fractions to come off the column were used for rapid-mixing measurements. Protein concentrations were determined using the molar absorption coefficient for 2-hydroperoxycoelenterazine bound within the aequorin ($\varepsilon_{460\ nm}$ = 1815 $cm^{-1}\ M^{-1}$ (5)).

The light response kinetics after sudden exposure to a saturating Ca^{2+} concentration was examined with an SX20 stopped-flow machine (cell volume 20 μL, dead time 1.1 ms) (Applied Photophysics, UK). The temperature was controlled with a circulating water bath and was set at 20°C in all experiments. The Ca^{2+} syringe contained 40 mM Ca^{2+}, 30 mM KCl, 5 mM PIPES buffer, pH 7.0. 2 μM of photoprotein was dissolved in a Ca^{2+}-free solution of the same ionic strength: 150 mM KCl, 5 mM PIPES, pH 7.0. Both syringes were prewashed with the EDTA solution and then, thoroughly, with deionized water. The solutions were mixed in equal volumes. Thus, the final concentrations of Ca^{2+} and photoprotein in the reaction mixture were 20 mM and 1 μM, respectively.

Kinetic analysis. Simulations were performed with the application made in SciLab environment supplied with built-in function *ode* for integration of differential equation systems. Nonlinear least squares fitting using Nelder–Mead optimization method built in the SciLab 5.4.1 was applied for finding the best solution. MSE (mean square error) and MAPE (mean absolute percentage errors) were used as a measure of the differences between values predicted by a model and the values observed in the experiments.

RESULTS AND DISCUSSION

Ca^{2+}-regulated photoproteins from different organisms demonstrate the same bioluminescence kinetic pattern. After rapid mixing with Ca^{2+} ions, photoproteins display a prompt increase of light signal, which reaches its peak within milliseconds. A flash in bioluminescence intensity is followed by a slow decay of the

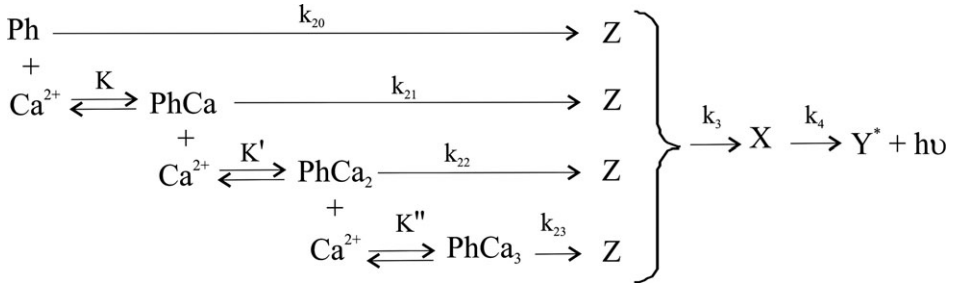

Scheme 2. Reaction scheme for obelin bioluminescence (48).

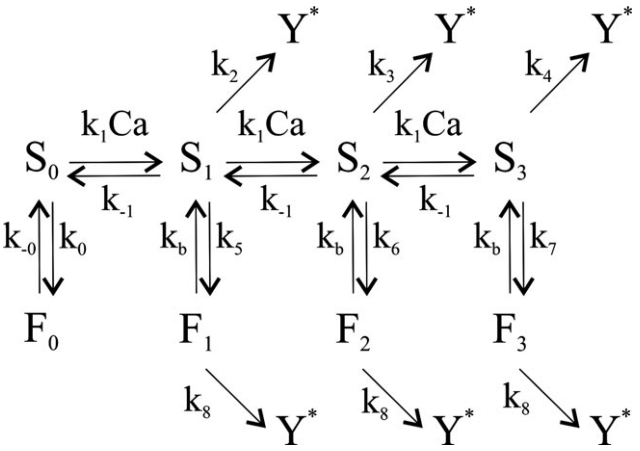

Scheme 3. Kinetic scheme for aequorin bioluminescence with "fast" and "slow" photoprotein forms (49).

light emission, lasting seconds. The decay rate is shown to increase with Ca^{2+} concentration, whereas the total light emitted (light integral) remains relatively constant (45,51). However, the rates of rise of light intensity and decay of bioluminescence signal significantly vary among Ca^{2+}-regulated photoproteins (44) and also depend on whether native coelenterazine or its various analogues are used for the activation of photoprotein (52). In addition, photoprotein bioluminescence kinetics might be affected by substitution of certain residues situated within substrate-binding cavity (37,38). For instance, the replacement of Trp92 to Phe which is located within hydrogen bond distance to the 6-(p-hydroxy)-phenyl group in obelin increases the rate of rise of light signal more than two times as compared to wild-type obelin (37).

In order to propose a general kinetic scheme describing bioluminescence signals of photoproteins from different organisms, several models were tested. The appropriate model was selected from comparison of simulated traces with experimental kinetic data.

Foremost, we examined kinetic schemes suggested for aequorin and obelin (see Supporting information for details). Simulation with the simple consecutive model based on Scheme 1 suggested for aequorin (45) was found to give an unsatisfactory fit to the experimental kinetic curves (MAPE = 20.79%; Fig. S1).

The kinetic model suggested for obelin bioluminescence (Scheme 2) (48), in effect, is an extended consecutive model suggested earlier for aequorin (45,47). This model additionally takes into account the ability of photoproteins to emit light in the absence of calcium ions and admits the light emission from photoprotein intermediates with occupied one, two and three Ca^{2+}-binding sites (48). This assumption is consistent with experimental results obtained for obelin mutants with disabled Ca^{2+}-binding sites (53). Simulation using this model also does not provide a satisfactory fit to the experimental kinetic curves (MAPE = 15.4%; Fig. S2).

Another model tested (Scheme 3) was recently suggested for aequorin bioluminescence (49). It was speculated that there are at least two fractions of photoproteins present, which can yield subsequent intermediates with different rate constants after calcium binding. The very possibility that each of the sites to which calcium binds has two states was suggested long ago (46). However, in contrast to the so-called dark state proposed in Allen *et al.* (46), both photoprotein states from Scheme 3 yield the "light-effective" intermediates and might be considered to be "fast" and "slow" components of the reaction due to their kinetics properties. Aside from two photoprotein forms, the model also admits the triggering light emission by binding of only one and two calcium ions to the photoprotein molecule (Scheme 3) similar to the model proposed for obelin (Scheme 2). The simulation traces became only slightly better fitted with experimental data when "fast" and "slow" photoprotein states (Scheme 3) were added into consideration (MAPE = 20.58%; Fig. S3).

All Ca^{2+}-regulated photoproteins have the same compact globular structure consisting of two sets of four helices comprising helix-turn-helix motifs known as EF-hands forming *N*- and *C*-terminal protein domains. Thus, the overall structure of photoprotein is seen as two "cups" joined at their rims (Fig. 1a). The 2-hydroperoxycoelenterazine molecule is situated in an internal cavity formed by residues located in all helices. In EF-hand proteins, the EF-hand motif almost always occurs in pairs. In the *N*-terminal domain, the EF-hand motif I is paired with EF-hand motif II, which displays the characteristic structural features of an EF-hand motif but has no canonical sequence in the loop for

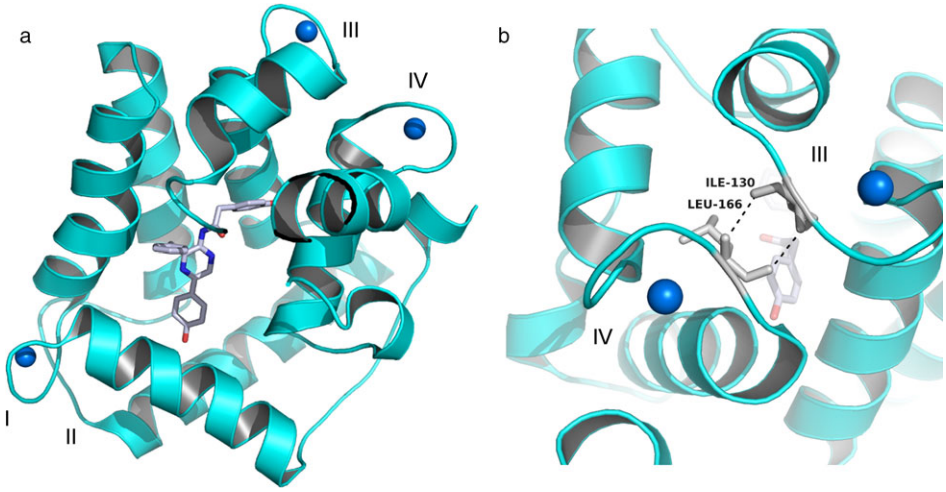

Figure 1. Spatial structure of Ca^{2+}-discharged obelin (PDB code 2F8P) (a) and interaction between EF-hand motifs III and IV Ca^{2+}-binding loops (b).

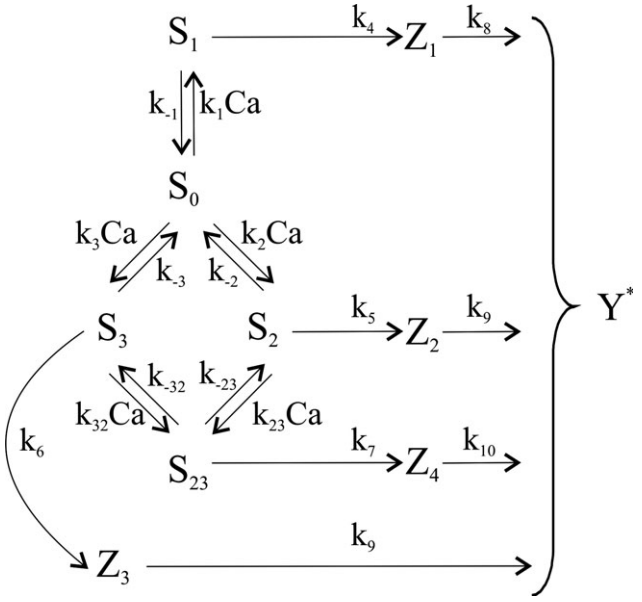

Scheme 4. Kinetic scheme of photoprotein bioluminescence with addition of Ca^{2+}-cooperativity effect.

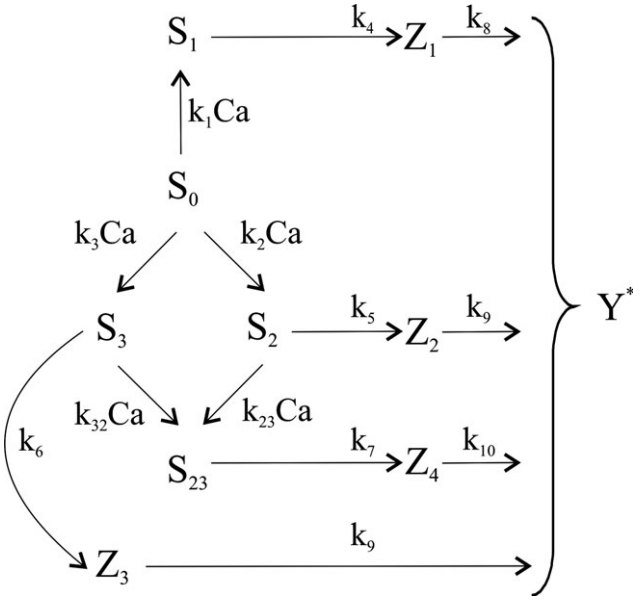

Scheme 5. Kinetic scheme of photoprotein bioluminescence with addition of Ca^{2+}-cooperativity effect without reverse rate constants.

calcium binding and consequently does not bind Ca^{2+} (54). The *C*-terminal domain is formed by EF-hand motifs III and IV. The Ca^{2+}-binding loops of these motifs having canonical 12-residue sequences interact with each other through hydrogen bonds (Fig. 1b). Frequently, the paired EF-hand motifs are capable of binding calcium ions with positive cooperativity, that is Ca^{2+}

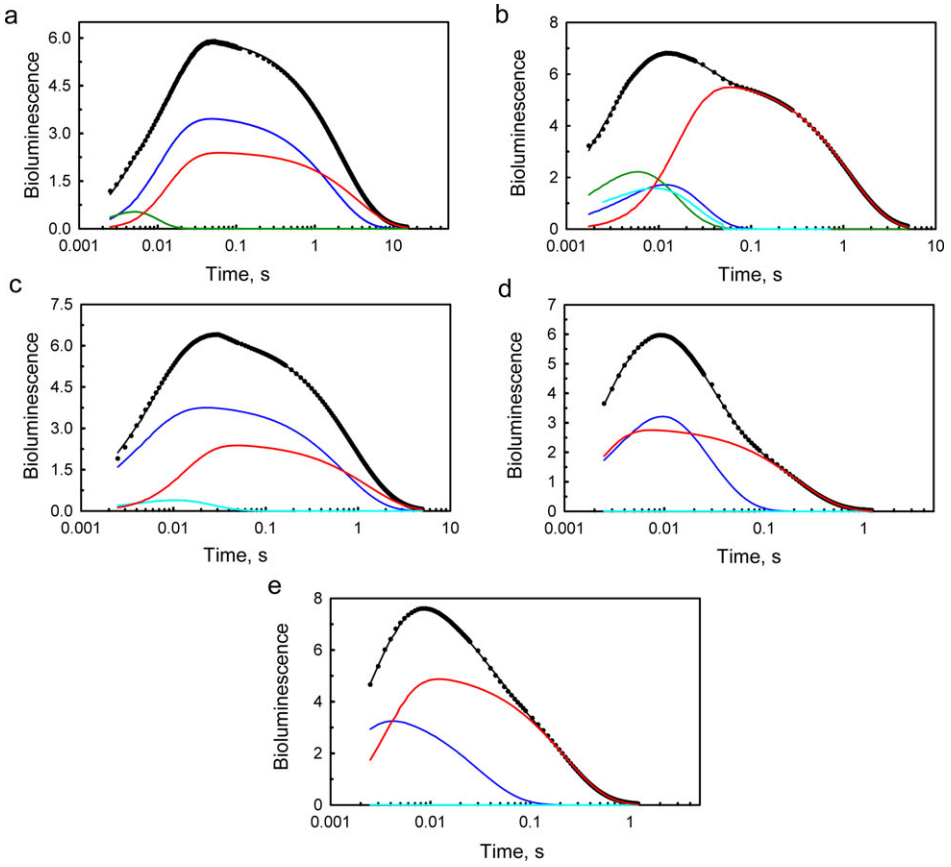

Figure 2. Stopped-flow records of luminescence signal for aequorin (a), clytin (b), mitrocomin (c) and obelins from *Obelia longissima* (d) and *Obelia geniculata* (e). Experimental traces are shown as black dots; traces modeled with Scheme 5—as black line, intermediate Z_1—as blue line, intermediate Z_2—as green line, intermediate Z_3—as cyan line and intermediate Z_4—as red line.

binding with one of the Ca^{2+}-binding sites increases affinity of another Ca^{2+}-binding site (55). Thus, a small change in calcium concentration might initiate structural and functional response of Ca^{2+}-binding proteins. Since spatial organization of EF-hand motifs in the *C*-terminal domain of photoproteins completely corresponds to that in other Ca^{2+}-binding proteins which display positive cooperativity, we can reasonably assume that at least the Ca^{2+}-binding sites situated in the *C*-terminal domain of Ca^{2+}-regulated photoproteins are also capable of binding calcium with positive cooperativity. Of note is that in case of photoproteins, small changes in calcium concentration stimulate high changes in bioluminescence intensity; the increase of $[Ca^{2+}]$ from 10^{-8} to 10^{-3} M leads to gain of light intensity by 7–8 orders of magnitude. Hence, we believe that the "positive cooperativity" must be introduced into photoprotein reaction scheme.

Since none of the considered models gave a satisfactory matching of simulated traces to experimental data (Figs S1–S3), we propose another kinetic model for the photoprotein bioluminescence reaction (Scheme 4).

To begin with, in this kinetic scheme, we added the "positive cooperativity" effect between Ca^{2+}-binding sites of the C-terminal domain (state S_{23} leading to the intermediate Z_4). We also admit that an excited state Y* could be formed as the result of binding of only one calcium ion to any of the Ca^{2+}-binding sites, which gives us intermediates Z_1, Z_2 and Z_3. In addition, in this scheme we neglected the Ca^{2+}-independent luminescence from S_0 due to the extremely low emission level compared to the Ca^{2+}-induced bioluminescence (46). Moreover, since in our experimental setup all five photoproteins were tested under saturating calcium concentration, it is reasonable to simplify the kinetic scheme by neglecting the reverse rate constants for all calcium-binding steps (Scheme 5).

The system of differential equation for Scheme 5:

$$\begin{cases} S_0 = -k_{-1}CS_0 - k_2CS_0 - k_3CS_0 - k_0S_0 \\ S_1 = k_1CS_0 - k_4S_1 \\ S_2 = k_2CS_0 - k_{23}CS_2 - k_5S_2 \\ S_3 = k_3CS_0 - k_{32}CS_3 - k_6S_3 \\ S_{23} = k_{23}CS_2 + k_{32}CS_3 - k_7S_{23} \\ Z_1 = k_0S_0 + k_4S_1 - k_8Z_1 \\ Z_2 = k_5S_2 - k_9Z_2 \\ Z_3 = k_6S_3 - k_9Z_3 \\ Z_4 = k_7S_{23} - k_{10}Z_4 \end{cases}$$

Simulations showed that usage of Scheme 5 as a photoprotein reaction model gives a good fit to the experimental data for all five photoproteins (Fig. 2); MAPE values are less than 5% which is much better than those of original models (48,49) (see Supporting information section). Rate constants obtained from the fits of experimental kinetic curves to the model presented in

Table 1. Bioluminescence rate constants of Ca^{2+}-regulated photoproteins from the raw kinetic curves.

	Aequorin	Clytin	Mitrocomin	Obelin-*l*	Obelin-*g*
k_1, $\times 10^4$ M^{-1} s^{-1}	0.685	0.83	17.2	2.37	0.638
k_2, $\times 10^5$ M^{-1} s^{-1}	0.05	5.77	1.0	0.63	0.33
k_3, $\times 10^5$ M^{-1} s^{-1}	0.05	4.25	1.0	0.63	0.33
k_{23}, $\times 10^4$ M^{-1} s^{-1}	2.15	0.46	0.69	5.0	5.0
k_{32}, $\times 10^4$ M^{-1} s^{-1}	2.15	0.68	0.69	5.0	5.0
k_4, s^{-1}	0.605	65.2	1.41	40.1	34.2
k_5, s^{-1}	0.5	0.97	1.02	0.15	0.05
k_6, s^{-1}	0.5	1.08	1.0	0.15	0.05
k_7, s^{-1}	0.283	0.85	0.78	4.62	4.60
k_8, s^{-1}	118	109	226	229	1100
k_9, s^{-1}	433	288	66.6	201	599
k_{10}, s^{-1}	107	137	164	1140	468
MSE, $\times 10^{-4}$	4.08	7.46	4.37	2.9	6.7
MAPE, %	3.89	2.94	1.7	4.4	4.54

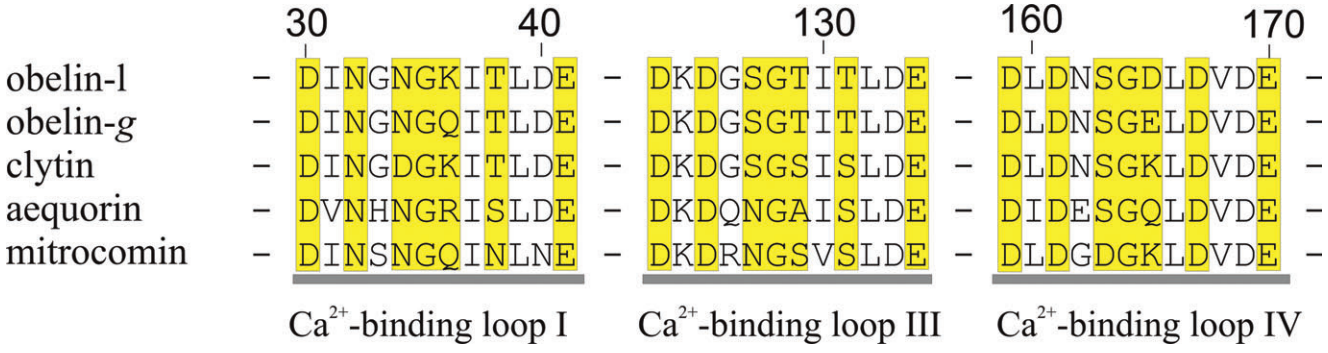

Figure 3. Multiple sequence alignment of Ca^{2+}-binding sites among different Ca^{2+}-regulated photoproteins: aequorin from *Aequorea victoria*, clytin from *Clytia gregaria*, mitrocomin from *Mitrocoma cellularia* and obelins from *Obelia longissima* and *Obelia geniculata*. Calcium-binding loops I, III and IV are shown as gray underbars. The calcium-binding consensus sequences within the loops are marked in yellow.

Scheme 5 are summarized in Table 1. The kinetic characteristics of the bioluminescence reactions of five photoproteins show considerable differences in rate constants. For example, according to Scheme 5, binding of calcium ions to the N-terminal Ca^{2+}-binding site (S_1) governed by k_1 is considerably faster in case of mitrocomin and equals to 17.2×10^4 M^{-1} s^{-1}. As for the C-terminal Ca^{2+}-binding sites (S_2 and S_3), corresponding rate constants k_2 and k_3 are the same for each photoprotein because we cannot distinguish these two sites in the model and therefore consider them as equivalent binding sites. Clytin displays the highest values of second-order rate constants k_2 and k_3, while aequorin shows the lowest rate of calcium binding to the C-terminal Ca^{2+}-binding sites—4.25–5.77 $\times 10^5$ M^{-1} s^{-1} and 0.05×10^5 M^{-1} s^{-1}, respectively. Ca^{2+}-binding sites III and IV contain polar Ser and Thr residues in all photoproteins (Fig. 3), which might be linked to the fast binding of calcium, while only aequorin has less polar amino acid residues such as Ala and Gln as well as Glu in the corresponding Ca^{2+}-binding sites. Formation of the photoprotein state with two calcium ions bound with cooperative effect (S_{23}) is governed by k_{23} and k_{32} which rate constants are also undistinguishable in our model. As for the values of k_{23} and k_{32}, all photoproteins used in our experiments can be divided into two groups: clytin and mitrocomin having the lowest rates of S_{23} formation—around 0.46–0.69 $\times 10^4$ M^{-1} s^{-1}—and aequorin and both obelins with k_{23} and k_{32} around 2–5 $\times$ M^{-1} s^{-1}. Mitrocomin and clytin Ca^{2+}-binding sites III contain Ser instead of Ala and Thr, and in the Ca^{2+}-binding site IV, they have Lys residues instead of Gln, Asp and Glu found at the same positions in the sequence of aequorin and obelins, respectively (Fig. 3). This might be the reason for the decreased positive cooperativity effect we observe in case of mitrocomin and clytin.

In Scheme 5, there are four intermediate states of photoproteins depending on the number and order of calcium ions bound —Z_1 (one calcium ion in N-terminal binding site), Z_2 and Z_3 (one calcium ion bound to one of the *C*-terminal Ca^{2+}-binding sites), and Z_4 (two calcium ions occupied in both *C*-terminal Ca^{2+}-binding sites). Separate kinetic traces for generation of these four intermediates are shown in Fig. 2 as color lines (see legend). All photoproteins can be divided into two groups according to the rate of Z_1 formation (Table 1). Clytin and two obelins represent a "fast" group with first-order rate constant k_4 in range 34.2–65.2 s^{-1}, and aequorin and mitrocomin are in a "slow" group where k_4 equals to 0.605 s^{-1} and 1.41 s^{-1}, respectively. The observed difference can be explained by the fact that both obelins and clytin have Thr, whereas aequorin—Ser and mitrocomin—Asn in Ca^{2+}-binding site I (Fig. 3). The rate of Z_2 and Z_3 formation is similar in case of aequorin, clytin and mitrocomin—0.5–1.08 s^{-1}, but considerably different in case of obelins—almost 10 times lower (0.05 s^{-1} for obelin-*g* and 0.15 s^{-1} for obelin-*l*). However, both obelins display the highest rates of Z_4 formation—4.60 s^{-1}, which are 5–15 times faster than those of the other photoproteins. This is probably because the *C*-terminal Ca^{2+}-binding sites of obelins are characterized with higher positive cooperativity than those of clytin and mitrocomin, 0.85 s^{-1} and 0.78 s^{-1}, respectively, let alone aequorin—0.283 s^{-1}.

As for the excited state Y* formation, there are also considerable differences in the rate constants for all five photoproteins depending on the type of intermediate Z it is formed from (Table 1). The biggest difference is between k_8 values for slow photoproteins (aequorin and clytin) and obelin-*g*, which is one order of magnitude—118 s^{-1}, 109 s^{-1} and 1100 s^{-1}, respectively.

CONCLUSION

In the present work, we propose a unanimous kinetic model describing the bioluminescence reaction of Ca^{2+}-regulated photoproteins based on rapid-mixing kinetic studies of five photoproteins: aequorin from *A. victoria*, clytin from *C. gregaria*, mitrocomin from *M. cellularia* and obelins from *O. longissima* and *O. geniculata.* The reaction scheme suggested includes a "positive cooperativity" effect between Ca^{2+}-binding sites of the *C*-terminal domain and takes into account the fact that an excited state Y* could be formed as the result of binding of only one calcium ion to any of the Ca^{2+}-binding sites. The kinetic model proposed in the present study provides a very good fit to the experimental rapid-mixing curves for all five photoproteins tested under saturating calcium concentration and provides a solid basis for the further study on details of emitters' formation.

Acknowledgements—This work was supported by RFBR grant 14-04-31092 and the state budget allocated to the fundamental research at the Russian Academy of Sciences (projects 01201351504 and 01201351502).

SUPPORTING INFORMATION

Additional Supporting Information may be found in the online version of this article:

Figure S1 Aequorin kinetic curve (black dots) fitted to Scheme 1 (red line).

Figure S2 Obelin-*g* kinetic curve (black dots) fitted to Scheme 2 (red line).

Figure S3 Aequorin kinetic curve (black dots) fitted to Scheme 3 (red line).

REFERENCES

1. Shimomura, O. and F. H. Johnson (1978) Peroxidized coelenterazine, the active group in the photoprotein aequorin. *Proc. Natl Acad. Sci. USA* **75**, 2611–2615.
2. Head, J. F., S. Inouye, K. Teranishi and O. Shimomura (2000) The crystal structure of the photoprotein aequorin at 2.3 Å resolution. *Nature* **405**, 372–376.
3. Liu, Z. J., E. S. Vysotski, L. Deng, J. Lee, J. Rose and B. C. Wang (2003) Atomic resolution structure of obelin: Soaking with calcium enhances electron density of the second oxygen atom substituted at the C2-position of coelenterazine. *Biochem. Biophys. Res. Commun.* **311**, 433–439.
4. Vysotski, E. S. and J. Lee (2004) Ca^{2+}-regulated photoproteins: Structural insight into the bioluminescence mechanism. *Acc. Chem. Res.* **37**, 405–415.
5. Shimomura, O. (2006) *Bioluminescence: Chemical Principles and Methods*. World Scientific Publishing, Singapore.
6. Prasher, D., R. O. McCann and M. J. Cormier (1985) Cloning and expression of the cDNA coding for aequorin, a bioluminescent calcium-binding protein. *Biochem. Biophys. Res. Commun.* **126**, 1259–1268.
7. Inouye, S., M. Noguchi, Y. Sakaki, Y. Takagi, T. Miyata, S. Iwanaga, T. Miyata and F. I. Tsuji (1985) Cloning and sequence analysis of cDNA for the luminescent protein aequorin. *Proc. Natl Acad. Sci. USA* **82**, 3154–3158.
8. Prasher, D. C., R. O. McCann, M. Longiaru and M. J. Cormier (1987) Sequence comparisons of complementary DNAs encoding aequorin isotypes. *Biochemistry* **26**, 1326–1332.
9. Gurskaya, N. G., A. F. Fradkov, N. I. Pounkova, D. B. Staroverov, M. E. Bulina, Y. G. Yanushevich, Y. A. Labas, S. Lukyanov and K.

A. Lukyanov (2003) A colourless green fluorescent protein homologue from the nonfluorescent hydromedusa *Aequorea coerulescens* and its fluorescent mutants. *Biochem. J.* **373**, 403–408.
10. Xia, N. S., W. X. Luo, J. Zhang, X. Y. Xie, H. J. Yang, S. W. Li, M. Chen and M. H. Ng (2002) Bioluminescence of *Aequorea macrodactyla*, a common jellyfish species in the East China Sea. *Mar. Biotechnol.* **4**, 155–162.
11. Inouye, S. and F. I. Tsuji (1993) Cloning and sequence analysis of cDNA for the Ca^{2+}-activated photoprotein, clytin. *FEBS Lett.* **315**, 343–346.
12. Inouye, S. (2008) Cloning, expression, purification and characterization of an isotype of clytin, a calcium-binding photoprotein from the luminous hydromedusa *Clytia gregarium*. *J. Biochem.* **143**, 711–717.
13. Markova, S. V., L. P. Burakova, L. A. Frank, S. Golz, K. A. Korostileva and E. S. Vysotski (2010) Green-fluorescent protein from the bioluminescent jellyfish *Clytia gregaria*: cDNA cloning, expression, and characterization of novel recombinant protein. *Photochem. Photobiol. Sci.* **9**, 757–765.
14. Fourrage, C., K. Swann, J. R. Gonzalez Garcia, A. K. Campbell and E. Houliston (2014) An endogenous green fluorescent protein-photoprotein pair in *Clytia hemisphaerica* eggs shows co-targeting to mitochondria and efficient bioluminescence energy transfer. *Open Biol.* **4**, 130206.
15. Illarionov, B. A., S. V. Markova, V. S. Bondar, E. S. Vysotski and J. I. Gitelson (1992) Cloning and expression of cDNA for the Ca^{2+}-activated photoprotein obelin from the hydroid polyp *Obelia longissima*. *Dokl. Akad. Nauk* **326**, 911–913.
16. Illarionov, B. A., V. S. Bondar, V. A. Illarionova and E. S. Vysotski (1995) Sequence of the cDNA encoding the Ca^{2+}-activated photoprotein obelin from the hydroid polyp *Obelia longissima*. *Gene* **153**, 273–274.
17. Markova, S. V., E. S. Vysotski, J. R. Blinks, L. P. Burakova, B. C. Wang and J. Lee (2002) Obelin from the bioluminescent marine hydroid *Obelia geniculata*: Cloning, expression, and comparison of some properties with those of other Ca^{2+}-regulated photoproteins. *Biochemistry* **41**, 2227–2236.
18. Fagan, T. F., Y. Ohmiya, J. R. Blinks, S. Inouye and F. I. Tsuji (1993) Cloning, expression and sequence analysis of cDNA for the Ca^{2+}-binding photoprotein, mitrocomin. *FEBS Lett.* **333**, 301–305.
19. Burakova, L. P., P. V. Natashin, S. V. Markova, E. V. Eremeeva, N. P. Malikova, C. Cheng, Z. J. Liu and E. S. Vysotski (2016) Mitrocomin from the jellyfish *Mitrocoma cellularia* with deleted *C*-terminal tyrosine reveals a higher bioluminescence activity compared to wild type photoprotein. *J. Photochem. Photobiol., B*, **162**, 286–297.
20. Markova, S. V., L. P. Burakova, S. Golz, N. P. Malikova, L. A. Frank and E. S. Vysotski (2012) The light-sensitive photoprotein berovin from the bioluminescent ctenophore *Beroe abyssicola*: A novel type of Ca^{2+}-regulated photoprotein. *FEBS J.* **279**, 856–870.
21. Aghamaali, M. R., V. Jafarian, R. Sariri, M. Molakarimi, B. Rasti, M. Taghdir, R. H. Sajedi and S. Hosseinkhani (2011) Cloning, sequencing, expression and structural investigation of mnemiopsin from *Mnemiopsis leidyi*: An attempt toward understanding Ca^{2+}-regulated photoproteins. *Protein J.* **30**, 566–574.
22. Jafarian, V., R. Sariri, S. Hosseinkhani, M. R. Aghamaali, R. H. Sajedi, M. Taghdir and S. Hassannia (2011) A unique EF-hand motif in mnemiopsin photoprotein from *Mnemiopsis leidyi*: Implication for its low calcium sensitivity. *Biochem. Biophys. Res. Commun.* **413**, 164–170.
23. Powers, M. L., A. G. McDermott, N. C. Shaner and S. H. Haddock (2013) Expression and characterization of the calcium-activated photoprotein from the ctenophore *Bathocyroe fosteri*: Insights into light-sensitive photoproteins. *Biochem. Biophys. Res. Commun.* **431**, 360–366.
24. Shimomura, O. and F. H. Johnson (1975) Regeneration of the photoprotein aequorin. *Nature* **256**, 236–238.
25. Eremeeva, E. V., S. V. Markova, A. H. Westphal, A. J. Visser, W. J. van Berkel and E. S. Vysotski (2009) The intrinsic fluorescence of apo-obelin and apo-aequorin and use of its quenching to characterize coelenterazine binding. *FEBS Lett.* **583**, 1939–1944.
26. Eremeeva, E. V., P. V. Natashin, L. Song, Y. Zhou, W. J. van Berkel, Z. J. Liu and E. S. Vysotski (2013) Oxygen activation of apo-obelin-coelenterazine complex. *ChemBioChem* **14**, 739–745.
27. Ridgway, E. B. and C. C. Ashley (1967) Calcium transients in single muscle fibers. *Biochem. Biophys. Res. Commun.* **29**, 229–234.
28. Vysotski, E. S., S. V. Markova and L. A. Frank (2006) Calcium-regulated photoproteins of marine coelenterates. *Mol. Biol.* **40**, 355–367.
29. Nakajima-Shimada, J., H. Iida, F. I. Tsuji and Y. Anraku (1991) Monitoring of intracellular calcium in *Saccharomyces cerevisiae* with an apoaequorin cDNA expression system. *Proc. Natl Acad. Sci. USA* **88**, 6878–6882.
30. Bonora, M., C. Giorgi, A. Bononi, S. Marchi, S. Patergnani, A. Rimessi, R. Rizzuto and P. Pinton (2013) Subcellular calcium measurements in mammalian cells using jellyfish photoprotein aequorin-based probes. *Nat. Protoc.* **8**, 2105–2118.
31. Bruton, J. D., A. J. Cheng and H. Westerblad (2012) Methods to detect Ca^{2+} in living cells. *Adv. Exp. Med. Biol.* **740**, 27–43.
32. Whitaker, M. (2010) Genetically encoded probes for measurement of intracellular calcium. *Methods Cell Biol.* **99**, 153–182.
33. Koldenkova, V. P. and T. Nagai (2013) Genetically encoded Ca^{2+} indicators: Properties and evaluation. *Biochim. Biophys. Acta* **1833**, 1787–1797.
34. Deng, L., S. V. Markova, E. S. Vysotski, Z. J. Liu, J. Lee, J. Rose and B. C. Wang (2004) Crystal structure of a Ca^{2+}-discharged photoprotein: Implications for mechanisms of the calcium trigger and bioluminescence. *J. Biol. Chem.* **279**, 33647–33652.
35. Deng, L., E. S. Vysotski, S. V. Markova, Z. J. Liu, J. Lee, J. Rose and B. C. Wang (2005) All three Ca^{2+}-binding loops of photoproteins bind calcium ions: The crystal structures of calcium-loaded apo-aequorin and apo-obelin. *Protein Sci.* **14**, 663–675.
36. Liu, Z. J., G. A. Stepanyuk, E. S. Vysotski, J. Lee, S. V. Markova, N. P. Malikova and B. C. Wang (2006) Crystal structure of obelin after Ca^{2+}-triggered bioluminescence suggests neutral coelenteramide as the primary excited state. *Proc. Natl Acad. Sci. USA* **103**, 2570–2575.
37. Vysotski, E. S., Z. J. Liu, S. V. Markova, J. R. Blinks, L. Deng, L. A. Frank, M. Herko, N. P. Malikova, J. P. Rose, B. C. Wang and J. Lee (2003) Violet bioluminescence and fast kinetics from W92F obelin: Structure-based proposals for the bioluminescence triggering and the identification of the emitting species. *Biochemistry* **42**, 6013–6024.
38. Natashin, P. V., W. Ding, E. V. Eremeeva, S. V. Markova, J. Lee, E. S. Vysotski and Z. J. Liu (2014) Structures of the Ca^{2+}-regulated photoprotein obelin Y138F mutant before and after bioluminescence support the catalytic function of a water molecule in the reaction. *Acta Crystallogr. D Biol. Crystallogr.* **70**, 720–732.
39. Natashin, P. V., S. V. Markova, J. Lee, E. S. Vysotski and Z. J. Liu (2014) Crystal structures of the F88Y obelin mutant before and after bioluminescence provide molecular insight into spectral tuning among hydromedusan photoproteins. *FEBS J.* **281**, 1432–1445.
40. Ohmiya, Y., M. Ohashi and F. I. Tsuji (1992) Two excited states in aequorin bioluminescence induced by tryptophan modification. *FEBS Lett.* **301**, 197–201.
41. Stepanyuk, G. A., S. Golz, S. V. Markova, L. A. Frank, J. Lee and E. S. Vysotski (2005) Interchange of aequorin and obelin bioluminescence color is determined by substitution of one active site residue of each photoprotein. *FEBS Lett.* **579**, 1008–1014.
42. Eremeeva, E. V., S. V. Markova, L. A. Frank, A. J. Visser, W. J. van Berkel and E. S. Vysotski (2013) Bioluminescent and spectroscopic properties of His-Trp-Tyr triad mutants of obelin and aequorin. *Photochem. Photobiol. Sci.* **12**, 1016–1024.
43. Eremeeva, E. V., S. V. Markova, W. J. van Berkel and E. S. Vysotski (2013) Role of key residues of obelin in coelenterazine binding and conversion into 2-hydroperoxy adduct. *J. Photochem. Photobiol., B* **127**, 133–139.
44. Malikova, N. P., L. P. Burakova, S. V. Markova and E. S. Vysotski (2014) Characterization of hydromedusan Ca^{2+}-regulated photoproteins as a tool for measurement of Ca^{2+} concentration. *Anal. Bioanal. Chem.* **406**, 5715–5726.
45. Hastings, J. W., G. Mitchell, P. H. Mattingly, J. R. Blinks and M. van Leeuwen (1969) Response of aequorin bioluminescence to rapid changes in calcium concentration. *Nature* **222**, 1047–1050.
46. Allen, D. G., J. R. Blinks and F. G. Prendergast (1977) Aequorin luminescence: Relation of light emission to calcium concentration – a calcium-independent component. *Science* **195**, 996–998.
47. Moisescu, D. G. and C. C. Ashley (1977) The effect of physiologically occurring cations upon aequorin light emission.

Determination of the binding constants. *Biochim. Biophys. Acta* **460**, 189–205.
48. Stephenson, D. G. and P. J. Sutherland (1981) Studies on the luminescent response of the Ca^{2+}-activated photoprotein, obelin. *Biochim. Biophys. Acta* **678**, 65–75.
49. Tricoire, L., K. Tsuzuki, O. Courjean, N. Gibelin, G. Bourout, J. Rossier and B. Lambolez (2006) Calcium dependence of aequorin bioluminescence dissected by random mutagenesis. *Proc. Natl Acad. Sci. USA* **103**, 9500–9505.
50. Vysotski, E. S., Z. J. Liu, J. Rose, B. C. Wang and J. Lee (2001) Preparation and X-ray crystallographic analysis of recombinant obelin crystals diffracting to beyond 1.1 Å. *Acta Crystallogr. D Biol. Crystallogr.* **57**, 1919–1921.
51. Illarionov, B. A., L. A. Frank, V. A. Illarionova, V. S. Bondar, E. S. Vysotski and J. R. Blinks (2000) Recombinant obelin: Cloning and expression of cDNA purification, and characterization as a calcium indicator. *Methods Enzymol.* **305**, 223–249.
52. Malikova, N. P., A. J. Borgdorff and E. S. Vysotski (2015) Semisynthetic photoprotein reporters for tracking fast Ca^{2+} transients. *Photochem. Photobiol. Sci.* **14**, 2213–2224.
53. Illarionov, B. A., V. A. Illarionova, V. S. Bondar, E. S. Vysotski and J. R. Blinks (2001) All three calcium-binding sites participate in the regulation of obelin luminescence. In *Bioluminescence and Chemiluminescence* (Edited by J. F. Case, P. J. Herring, B. H. Robison, S. H. D. Haddock, L. J. Kricka and P. E. Stanley), pp. 75–78. World Scientific, Singapore, Proceedings of the 11th International Symposium on Bioluminescence and Chemiluminescence, Monterey, California, USA, 6-10 September 2000.
54. Kretsinger, R. H. and S. Nakayama (1993) Evolution of EF-hand calcium-modulated proteins. IV. Exon shuffling did not determine the domain compositions of EF-hand proteins. *J. Mol. Evol.* **36**, 477–488.
55. Chazin, W. J. (2011) Relating form and function of EF-hand calcium binding proteins. *Acc. Chem. Res.* **44**, 171–179.